

# Preliminary results of the theranostic $^{47}\text{Sc}$ cyclotron proton-induced production with enriched $^{48}\text{Ti}$ , $^{49}\text{Ti}$ and $^{50}\text{Ti}$ targets

Liliana Mou<sup>1,\*</sup>, Lucia De Dominicis<sup>1,2</sup>, Sara Cisternino<sup>1</sup>, Ferid Haddad<sup>3</sup>, Matteo Camprostrini<sup>1</sup>, Valentino Rigato<sup>1</sup>, Juan Esposito<sup>1</sup>, and Gaia Pupillo<sup>1</sup>

<sup>1</sup>Istituto Nazionale di Fisica Nucleare, Laboratori Nazionali di Legnaro (INFN-LNL), Viale dell'Università 2, 35020 Legnaro, Padova, Italy

<sup>2</sup>Università degli Studi di Padova, Dipartimento di Fisica e Astronomia Galileo Galilei, Via F. Marzolo 8, 35131 Padova, Italy

<sup>3</sup>Nantes University and GIP ARRONAX, 1 Rue Aronnax, 44800 Saint-Herblain, France

**Abstract.** The scientific community interest in the production of the theranostic  $^{47}\text{Sc}$  is due to its medical favourable decay characteristics suitable for both SPECT imaging and therapeutic purposes. Considering the SPES cyclotron, this work is focused on the measurement of the  $^{48/49/50}\text{Ti}(p,x)^{47}\text{Sc}$  and  $^{46}\text{Sc}$  cross sections up to 70 MeV. In fact,  $^{46}\text{Sc}$  is the main co-produced contaminant, since it has a longer half-life than the theranostic  $^{47}\text{Sc}$ . Enriched  $^{48/49/50}\text{Ti}$  powder were deposited on aluminum backing by using the HIVIPP technique and the obtained targets were characterized by Elastic Back Scattering at the INFN-LNL. Experimental data are compared with the scarce literature and the TALYS results, obtained using the default parameters.

## 1 Introduction

$^{47}\text{Sc}$  is one of the radionuclides of interest in theranostics thanks to its  $\beta^-$  and  $\gamma$ -radiation (Table 1) which make it suitable for both therapeutic and diagnostic purposes. Currently, the limiting factor for clinical and preclinical studies with  $^{47}\text{Sc}$ -labeled radiopharmaceuticals is the lack of  $^{47}\text{Sc}$  availability; thus, the study of possible production routes is crucial. In the framework of the LARAMED (LABoratory of RADioisotopes for MEDicine) program, the PASTA (*Production with Accelerator of Sc-47 for Theranostic Applications*) [1,2] and REMIX (*Research on Emerging Medical radionuclides from the X-sections*) [3,4] projects, funded by INFN in 2017/2018 and 2021/2023 respectively, aim to study the  $^{47}\text{Sc}$  production cross section starting from different target materials, namely  $^{nat}\text{V}$ ,  $^{48}\text{Ti}$ ,  $^{49}\text{Ti}$  and  $^{50}\text{Ti}$ . Considering that the SPES cyclotron is able to provide proton beams with a tunable energy from 35 MeV up to 70 MeV, this work aims at providing a comprehensive knowledge of  $^{47}\text{Sc}$  production, to find out the best p-induced nuclear reaction that allows enough  $^{47}\text{Sc}$  production

---

\* e-mail: liliana.mou@lnl.infn.it

considering the simultaneous minimization of the co-production of all possible contaminants. Particular attention must be paid to the other Sc-isotopes since they cannot be chemically separated from  $^{47}\text{Sc}$ . Among the Sc-isotopes, the most critical is  $^{46}\text{Sc}$  since it has a longer half-life than  $^{47}\text{Sc}$  (Table 1).

The  $^{nat}\text{V}(p,x)^{xx}\text{Sc}$  nuclear reactions were already studied and published [5] while the preliminary  $^{48/49/50}\text{Ti}(p,x)^{xx}\text{Sc}$  cross sections will be presented in this manuscript. It is important to underline that up to now there are no experimental data on the EXFOR database [6,7] for the  $^{49}\text{Ti}(p,x)^{47}\text{Sc}$  cross section and only a few data sets are published for the  $^{50}\text{Ti}(p,x)^{47}\text{Sc}$  and  $^{48}\text{Ti}(p,2p)^{47}\text{Sc}$  reactions.

**Table 1.** Nuclear data of  $^{47}\text{Sc}$  and  $^{46}\text{Sc}$  radionuclides [8].

Isotope	Half-life	Energy [keV] (Intensity [%])	$\beta$ - mean energy [keV] (Intensity [%])
$^{47}\text{Sc}$	3.3492 d	159.381 (68.3)	162.0 (100)
$^{46}\text{Sc}$	83.79 d	889.277 (99.984) 1120.545 (99.987)	118.3 (100)

## 2 Materials and methods

### 2.1 Enriched $^{48/49/50}\text{Ti}$ targets

The first challenge of this work was the realization of the thin Ti targets; it was thus necessary to realize at LNL a dedicate experimental set-up. The chosen deposition technique for target manufacturing was the High Energy Vibrational Powder Plating (HIVIPP) [9–11] that exploits the phenomenon of vibrational motion of metallic particles in a static electric field. The process is realized in vacuum and it is suitable for the deposition of expensive enriched powders since it has high efficiency with a negligible material loss (Fig. 1). Figure 1 shows a simple scheme of the experimental set-up and a target realized with the Ti powder deposited on an aluminum support.

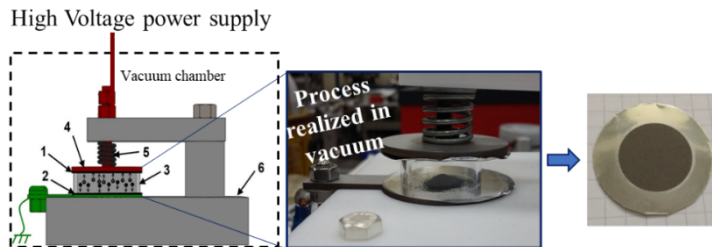


**Fig. 1.** Scheme and picture of the HIVIPP experimental set-up developed at INFN-LNL and a typical enriched Ti target.

For the cross section measurements is essential to know the exact quantity of material deposited ( $\text{mg}/\text{cm}^2$ ) on the aluminum support and, for this reason, the samples were analyzed by the Elastic Backscattering Spectrometry (EBS) at the LNL AN2000 Accelerator, using a proton beam of 1 mm diameter at 1.8 MeV and 10-20 nA current intensity. Each sample was analyzed in 3 different positions, in order to check also target homogeneity. Figure 2 shows a picture of the EBS experiments and a typical EBS

spectrum analysis. The deposited titanium is obtained from the fit (black line) of the experimental data (red dots), taking into account the contribution due to the presence of the aluminum substrate (blue line), titanium (gray line) and oxygen (purple line) due to the titanium oxidation, by minimizing the sum of the square difference between the calculated and measured channel values (Fig 2 right). The three spectra acquired in the three positions were always superimposable and this demonstrates the uniformity of the deposited Ti.

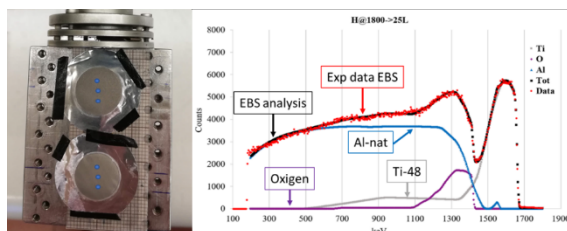


**Fig. 2.** Three different positions in which the EBS spectrum was acquired for each target (left) and an example of the analysis procedure of an EBS spectrum of  $^{48}\text{Ti}$  on Al target (right).

## 2.2 Irradiation runs and data analysis

As the dedicated LARAMED infrastructure is currently close to completion, the cross section measurements were performed in collaboration with the ARRONAX facility (Saint Herblain, France) [12]. The well-known stacked-foils target technique [13] was used, allowing for bombarding many target foils thus obtaining several cross section values at different energies in the same irradiation run. Typically, the irradiation runs had a duration of 60-90 minutes and a current of about 100 nA. In addition to an instrumented beam-dump,  $^{nat}\text{Ni}$  foils (10 or 25  $\mu\text{m}$  thick) were used for monitoring the beam flux through the stacked-target by referring to the  $^{nat}\text{Ni}(p,x)^{57}\text{Ni}$  monitor reaction recommended by the International Atomic Energy Agency (IAEA) [14]. At the end of each irradiation, the activated targets were measured via  $\gamma$ -spectrometry by using a High Purity Germanium Detectors (HPGe) previously calibrated with a reference  $^{152}\text{Eu}$  point-like solid source, provided by ARRONAX (purchased by CERCA-LEA, Site Nucléaire du Tricastin, France). The first  $\gamma$ -acquisition of each foil started 2-3 hours after the EOB and lasted for 15 minutes. In the days following the irradiation,  $\gamma$ -spectrometry measurements (usually 2-3 hours long) were carried out to follow the decay of the produced radionuclides. The cross sections, as a function of energy, and the associated errors were calculated by using the procedure described by N. Otuka et al. [15].

## 3 Results and Discussion

The preliminary experimental cross section values obtained for enriched  $^{48}\text{Ti}$ ,  $^{49}\text{Ti}$ , and  $^{50}\text{Ti}$  targets and for proton energy up to 70 MeV are shown in Figures 3-6. The TALYS code [16] was also used with default parameters to compare simulations with experimental values.

### 3.1 Cross section on $^{48}\text{Ti}$ targets

The data obtained for the  $^{48}\text{Ti}(p,x)^{47}\text{Sc}$ ,  $^{46}\text{Sc}$ , rescaled considering a 100% enriched target, are reported in Figure 3 and Figure 4. In the same graphs are also reported the data by Gadioli et al. (1981) [17] and Levkovskij (1991) [18], available from the EXFOR database. The data by Levkovskij were corrected by a factor of 0.8 due to the monitor values used in 1991 [19]; to indicate the applied rescaling factor a star is added in the legend (Fig. 3). A regular trend and a general good agreement between our new results and the literature data was found for both isotopes. It should be underlined that a discrepancy of up to 20% was found in the  $^{47}\text{Sc}$  production in the energy range 30-50 MeV, but at the same time there is a very good agreement for the  $^{46}\text{Sc}$  production. TALYS run with the default parameters overestimates the  $^{47}\text{Sc}$  production trend from  $^{48}\text{Ti}$  of approximately double between 30 and 70 MeV (Fig. 3), while it well reproduces the  $^{46}\text{Sc}$  production in the entire energy range investigated (Fig. 4). A dedicated paper describing all the details of this work, including also other co-produced isotopes (i.e.,  $^{48}\text{Ti}(p,x)^{44\text{m}}\text{Sc}$ ,  $^{44\text{g}}\text{Sc}$ ,  $^{43}\text{Sc}$  and  $^{48}\text{V}$ ), is currently under internal revision.

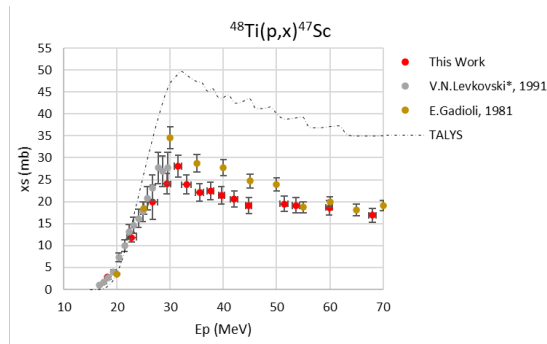


**Fig. 3.** Preliminary cross section of the  $^{48}\text{Ti}(p,2p)^{47}\text{Sc}$  nuclear reaction.

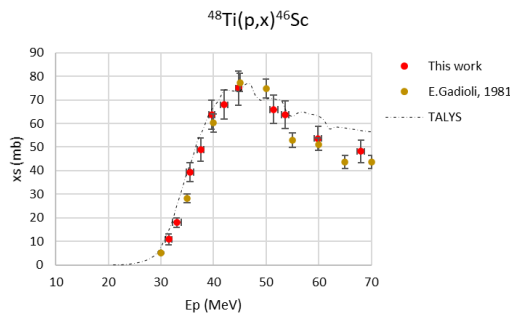


**Fig. 4.** Preliminary cross section of the  $^{48}\text{Ti}(p,x)^{46}\text{Sc}$  nuclear reaction.

### 3.2 Preliminary results on $^{49/50}\text{Ti}$ targets

The preliminary data obtained for the  $^{49/50}\text{Ti}(p,x)^{47}\text{Sc}$ ,  $^{46}\text{Sc}$  are reported in Figure 5 and Figure 6. Data are considered preliminary since they need the correction for:

- Exact amount of deposited enriched Ti from EBS analysis; cross sections were calculated considering only the weighting values of the samples before and after the HIVIPP deposition process.
- Isotopic composition of the enriched Titanium material; as reported in Table 2, the  $^{49}\text{Ti}$  data have to be corrected for 2.7% of  $^{48}\text{Ti}$ , while  $^{50}\text{Ti}$  data have to be corrected for 12.5% of  $^{48}\text{Ti}$  and 1.4% of  $^{49}\text{Ti}$ .

**Table 2.** Isotopic composition of enriched  $^{49}\text{Ti}$  and  $^{50}\text{Ti}$  purchased from Oak Ridge National Laboratory.

	Atomic Percent (precision)	
Isotope	Ti-49 powder	Ti-50 powder
46	0.220 (0.005)	1.69 (0.05)
47	0.220 (0.005)	1.29 (0.05)
48	2.710 (0.010)	12.51 (0.20)
49	96.250 (0.010)	1.41 (0.05)
50	0.600 (0.005)	83.10 (0.20)

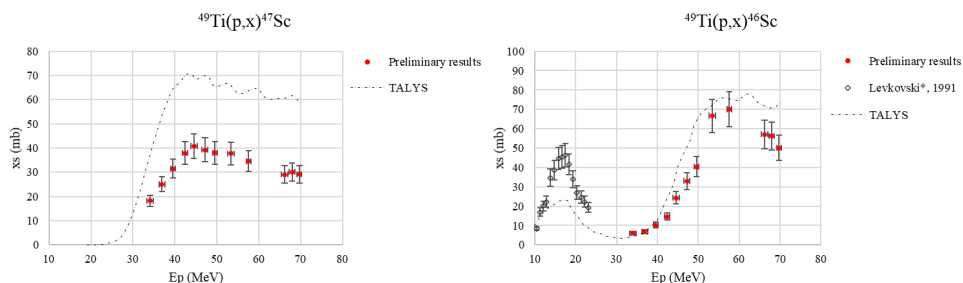


**Fig. 5.** Preliminary cross section of the  $^{49}\text{Ti}(p,x)^{47/46}\text{Sc}$  nuclear reactions.

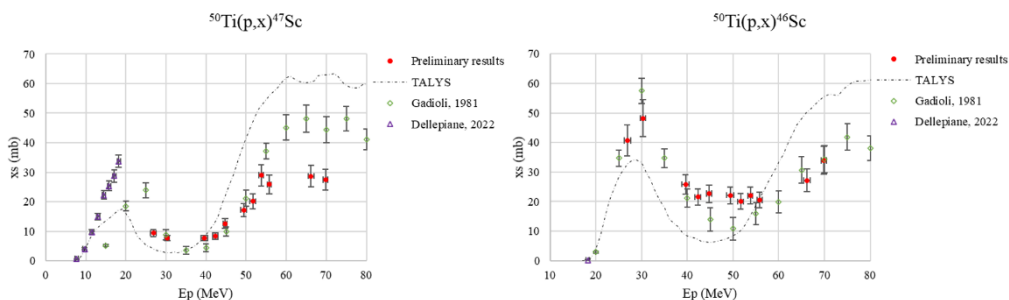


**Fig. 6.** Preliminary cross section of the  $^{50}\text{Ti}(p,x)^{47/46}\text{Sc}$  nuclear reactions.

Considering the corrections needed, any comment on the experimental data is quite premature. As already underlined, our data for the  $^{49}\text{Ti}(p,x)^{47}\text{Sc}$  reaction are the first available for the scientific community; the TALYS results seem to correctly describe the general trend of the reaction, with an overestimation of a factor of about 2. In the other cases, TALYS results seem to properly describe the experimental data, and a very good agreement can be noted for the  $^{49}\text{Ti}(p,x)^{46}\text{Sc}$  case.

In view of a potential clinical use of the  $^{47}\text{Sc}$  produced using  $^{49}\text{Ti}$  or  $^{50}\text{Ti}$  targets, dosimetric evaluations have to be performed to consider the contribution to the

additional dose due to the presence of contaminants (i.e.  $^{48}\text{Sc}$ ,  $^{46}\text{Sc}$ ,  $^{44g/44m}\text{Sc}$ ,  $^{43}\text{Sc}$ ) for different irradiation scenarios.

## 4 Conclusion

This work presents the experimental data of the  $^{48/49/50}\text{Ti}(p,x)^{47}\text{Sc}$ ,  $^{46}\text{Sc}$  cross sections. The  $^{48}\text{Ti}(p,x)^{47,46}\text{Sc}$  can be compared with the scarce literature values, while the  $^{49/50}\text{Ti}(p,x)$  data are still preliminary. However, the general trend of all the nuclear reactions studied in this work seems regular; additional work on TALYS estimations can be carried out to find the best physical parameters that better describe the experimental data. Once the final experimental data will be available, it will be possible to compare different  $^{47}\text{Sc}$  production scenarios to identify the best proton-induced reaction and energy range, considering the impurity profile of all co-produced Sc isotopes and their dosimetric impact for specific  $^{47}\text{Sc}$ -labelled radiopharmaceuticals [20].

## References

- [1] G. Pupillo, L. Mou, A. Boschi, S. Calzaferri, L. Canton, S. Cisternino, L. De Dominicis, A. Duatti, A. Fontana, F. Haddad, P. Martini, M. Pasquali, H. Skliarova, and J. Esposito, *J Radioanal Nucl Chem* **322**, 1711 (2019)
- [2] G. Pupillo, A. Fontana, L. Canton, F. Haddad, H. Skliarova, S. Cisternino, P. Martini, M. Pasquali, A. Boschi, J. Esposito, A. Duatti, and L. Mou, *Il Nuovo Cimento C* **42**, 1 (2019)
- [3] G. Pupillo, A. Boschi, S. Cisternino, L. De Dominicis, P. Martini, L. Mou, C. Rossi Alvarez, G. Sciacca, and J. Esposito, *J Radioanal Nucl Chem* (2023)
- [4] G. Pupillo, U. Anselmi-Tamburini, F. Barbaro, M. Bello, S. Bortolussi, A. Boschi, M. Campostrini, L. Canton, M. P. Carante, E. Cazzola, S. Cisternino, A. Colombi, M. Colucci, L. D. Dominicis, L. D. Nardo, A. Duatti, A. Fontana, G. Gorgoni, F. Groppi, F. Haddad, S. Manenti, P. Martini, L. Meléndez-Alafort, L. Mou, E. Nigrón, V. Rigato, G. Sciacca, and J. Esposito, *J. Phys.: Conf. Ser.* **2586**, 012118 (2023)
- [5] F. Barbaro, L. Canton, M. P. Carante, A. Colombi, L. De Dominicis, A. Fontana, F. Haddad, L. Mou, and G. Pupillo, *Phys. Rev. C* **104**, 044619 (2021)
- [6] V. V. Zerkin and B. Pritychenko, *Nuclear Instruments and Methods in Physics Research Section A: Accelerators, Spectrometers, Detectors and Associated Equipment* **888**, 31 (2018)
- [7] Experimental Nuclear Reaction Data (EXFOR), IAEA (n.d.)
- [8] NNDC, "National Nuclear Data Center NuDat (3.0) at Brookhaven National Laboratory" (n.d.)
- [9] H. Skliarova, S. Cisternino, L. Pranovi, L. Mou, G. Pupillo, V. Rigato, and C. Rossi Alvarez, *Nuclear Instruments and Methods in Physics Research Section A: Accelerators, Spectrometers, Detectors and Associated Equipment* **981**, 164371 (2020)
- [10] S. Cisternino, H. Skliarova, P. Antonini, J. Esposito, L. Mou, L. Pranovi, G. Pupillo, and G. Sciacca, *Instruments* **6**, 23 (2022)
- [11] S. Cisternino, L. De Dominicis, L. Mou, J. Esposito, C. Genanri, I. Calliari, and G. Pupillo, *Materials* **16**, (2023)

- [12] F. Haddad, L. Ferrer, A. Guertin, T. Carlier, N. Michel, J. Barbet, and J.-F. Chatal, *European Journal of Nuclear Medicine and Molecular Imaging* **35**, 1377 (2008)
- [13] G. Pupillo, L. Mou, P. Martini, M. Pasquali, A. Boschi, G. Cicoria, A. Duatti, F. Haddad, and J. Esposito, *Radiochimica Acta* **108**, 593 (2020)
- [14] IAEA - Monitor Reaction (n.d.)
- [15] N. Otuka, B. Lalremruata, M. U. Khandaker, A. R. Usman, and L. R. M. Punte, *Radiation Physics and Chemistry* **140**, 502 (2017)
- [16] A. Koning, S. Hilaire, and S. Goriely, *Eur. Phys. J. A* **59**, 131 (2023)
- [17] E. Gadioli, E. Gadioli Erba, J. J. Hogan, and K. I. Burns, *Zeitschrift Fur Physik A Hadrons and Nuclei* **301**, 289 (1981)
- [18] V. N. Levkovski, *Cross Sections of Medium Mass Nuclide Activation (A=40-100) by Medium Energy Protons and Alpha-Particles (E=10-50 MeV)* (Moscow, USSR, 1991)
- [19] S. Takács, F. Tárkányi, M. Sonck, and A. Hermanne, *Nuclear Instruments and Methods in Physics Research Section B: Beam Interactions with Materials and Atoms* **198**, 183 (2002)
- [20] L. De Nardo, G. Pupillo, L. Mou, D. Furlanetto, A. Rosato, J. Esposito, and L. Meléndez-Alafort, *Phys. Med. Biol.* **66**, 025003 (2021)